THE LANCET Neurology

Supplementary webappendix

This webappendix formed part of the original submission and has been peer reviewed. We post it as supplied by the authors.

Supplement to: Paulsen JS, Long JD, Ross CA, et al, and the PREDICT-HD Investigators and Coordinators of the Huntington Study Group. Prediction of manifest Huntington's disease with clinical and imaging measures: a prospective observational study. *Lancet Neurol* 2014; published online Nov 3. http://dx.doi.org/10.1016/S1474-4422(14)70238-8.

Variable descriptions

Lobar white = the sum of frontal, parietal, temporal, and occipital lobe white matter for both hemispheres divided by baseline intra-cranial volume (ICV).

Lobar gray = the sum of frontal, parietal, temporal, and occipital lobe gray matter for both hemispheres divided by baseline ICV.

CSF = cerebrospinal fluid divided by baseline ICV.

Hippo = hippocampus divided by baseline ICV.

Globus = globus pallidus divided by baseline ICV.

TMS = total motor score from the Unified Huntington Disease Rating Scale (UHDRS). Standardized ratings of oculomotor function, dysarthria, chorea, dystonia, gait and postural stability.[1]

Brady = bradykinesia subscale from the UHDRS. Rating of abnormal slowness or rigidity of movement.[1]

Ocular = ocular subscale from the UHDRS. Rating of eye movement and tracking.[1]

SDMT = Symbol Digit Modalities Test. The SDMT is an adaptation of the Wechsler Digit Symbol subtest that measures working memory, complex scanning, and processing speed.[2,3] Participants use a key presented at the top of the test page to match symbols with numbers presented in horizontal rows. The task requires that the participant fill in the appropriate symbols below the matching numbers as quickly as possible. Raw scores indicate the number of items correctly completed in 90 seconds.[4]

Stroop = Stroop Color and Word Test –consists of three 45-second trials.[5] The first two trials (color identification and word reading) measure basic attention and processing speed. In the first trial, participants must correctly identify the color of ink patches on a stimulus card. In the second trial, participants read the names of colors printed in black ink. In the third trial, the interference trial, participants must consistently inhibit an overlearned response by identifying the color of ink (red, green, blue) that the stimulus color words are printed in rather than reading the word aloud. Raw scores indicate the number of items correctly completed per trial.[6]

Timing = time production or paced tapping. Participants were presented with a 1·8 Hz tone and were instructed to tap along with it when ready. After 11 more presentations of the tone, the tone stopped, and participants attempted to continue to tap at the same pace for 31 more taps. The variable analyzed is the reciprocal of the standard deviation of the intertap interval for an alternating thumbs trial (smaller values indicate worse performance) over five trials.[7]

Sp-Tapping = speeded tapping. Finger tapping speed was assessed by calculating the mean intertap interval of five 10-second trials of tapping as quickly as possible with the nondominant finger (smaller values indicate better performance).[7]

Smell-ID = University of Pennsylvania Smell Identification Test (UPSIT). The smell identification test is a multiple-choice measure of olfactory recognition. Participants scratched a scented patch in a test booklet and identified the corresponding scent label from four multiple choice options.[8] Some participants completed the full four-booklet version of the UPSIT, others completed an abbreviated, 20-item version. The percentage of correctly identified scents was analyzed.[8]

TMT = Trail Making Test. In TMT-A, participants draw lines connecting numbered circles as quickly as possible. Raw scores indicate the number of seconds required to complete each test.[9,10] In TMT-B, participants alternate between connecting numbered and lettered circles according to ascending, alphabetical order (i.e., 1-A, 2-B, 3-C, etc.). Raw scores indicate the number of seconds required to complete each test.[9,10]

EmoRec = emotion recognition test. Emotion recognition was assessed by two emotion-labeling tasks.[11] One of the tasks employed static photographs of human faces, while the other used the same stimuli with simulated movement.[12] In both tasks, participants were asked to identify the emotion displayed by a target face. In the static condition, an expression of moderate intensity was presented for one second. The options were fear, disgust, happy, sad, surprise, anger, and neutral. In the simulated movement condition, an expression of mild intensity presented for 500 milliseconds transformed into an expression of moderate intensity for 500 milliseconds. The variables analyzed for each are the number of negative emotions correctly identified.[11,13]

TFC = total functional capacity from the UHDRS. A list of independent and common daily tasks that can be accomplished.[1]

ECog-C = Everyday Cognition Rating Scale – Companion Rating Scale. An adult familiar with the participant rates the participant's memory, language, semantic knowledge, visuospatial abilities, planning, organization, and divided attention.[14]

FAS = functional activity scale from the UHDRS.[1]

WHODAS-C = World Health Organization Disability Assessment Schedule – companion rating scale. A generic assessment for health and disability as related by a close companion.[15]

S-OC-C = Symptom Checklist 90 – obsessive compulsive scale – companion rating scale. A 90-item assessment taking 15 minutes to administer, with this subscale focusing on obsessive-compulsive disorders as rated by companions.[16]

F-Exc-C = Frontal Systems Behavioral Scale – executive subscale – companion rating scale. Part of a 46-item behavior rating scale focusing on abstraction, problem solving, and hypothesis generation as rated by a companion focusing on dorsolateral prefrontal circuitry.[17]

F-Apa-C = Frontal Systems Behavioral Scale – apathy subscale – companion rating scale. Part of a 46-item behavior rating scale associated with anterior cingulate circuitry.[17]

S-GSI-C = Symptom Checklist 90 – Global Severity Index – companion rating scale. A 90-item assessment taking 15 minutes to administer. Global severity is one of the three major indices.[16]

S-Dep-C = Symptom Checklist 90 – depression subscale – companion rating scale. A 90-item assessment taking 15 minutes to administer, with this subscale focusing on depressive symptoms as rated by companions.[16]

S-Anx-C = Symptom Checklist 90 – anxiety subscale – companion rating scale. A 90-item assessment taking 15 minutes to administer, with this subscale focusing on anxiety as rated by companions.[16]

BDI = Beck Depression Inventory–II. A 21-question inventory to measure the severity of depression.[18]

F-Dis-C = Frontal Systems Behavioral Rating Scale – disinhibition subscale – companion rating scale. Part of a 46-item scale associated with orbitofrontal circuitry.[17]

S-Hos-C = Symptom Checklist 90 – hostility subscale – companion rating scale. A 90-item assessment taking 15 minutes to administer with this subscale focusing on outward hostility toward others as rated by companions.[16]

Available measures and sample size variation

The initial National Institutes of Health study grant was funded from 2000-2003 and budgeted for 400 participants; the second grant was funded from 2004-2007 and budgeted for 650 participants; the third grant was funded from 2008-2013 and budgeted for 1000 participants. CHDI, Inc. funded the additional 300 participants. Participants could only be consented for the funded project for which they enrolled. We then invited their participation in the renewal grant when possible. We are fortunate that many (most) participants chose to continue in the study and our dropouts were less than initially calculated.

Several measures were introduced and discontinued throughout the study. PREDICT-HD was a natural history study designed to develop measures sensitive to disease progression in premanifest HD. When a specific measure was found to be less sensitive than

another, the task was discontinued (or modified) and another test was developed in its place. For example, it was found that the functional measures were not sensitive to premanifest HD (TFC and FAS) so we abbreviated them both by only administering the items which showed the earliest changes in premanifest HD (i.e., did not ask about toileting since it was always independent in premanifest HD). We then developed a new scale, the Work Function measure, to see if we could measure earlier functional declines. We have since published studies that show good sensitivity of the Work Function measure as an indicator of earlier functional decline in premanifest HD. Such tools will be critical should we choose to provide treatments before diagnosis. The Food and Drug Administration is likely to request evidence of outcomes important to the individual and showing functional impact.

Heterogeneity of Total Motor Score

As discussed in the text, relatively wide variability was observed in the TMS. Figure S1 shows the bar graph of the TMS at conversion (time=0) for the *N*=225 converters. Early in PREDICT-HD, substantial TMS variation was noted and the following efforts were made to assure data integrity: 1) new standardized training and certification criteria were immediately implemented into the study in the first few years; new videotapes were made by the European Huntington's Disease Network and new certification guidelines were mandated for all motor raters; 2) all motor examinations were videotaped and all tapes are digitized and archived for further viewing and analyses; 3) all outliers and extreme ranges were queried by the data management staff directly to the sites and motor raters; and 4) experienced motor raters were invited to view videotapes and discuss efforts to improve standardized motor ratings for clinical trials. It is our intent to continue to make this database available for further analyses and to continue to encourage the leaders in our field to provide guidance on improved reliability and validity of motor ratings for HD. From our study perspective, however, these are real data that have undergone quality assurance and quality control and the data are as we report them.

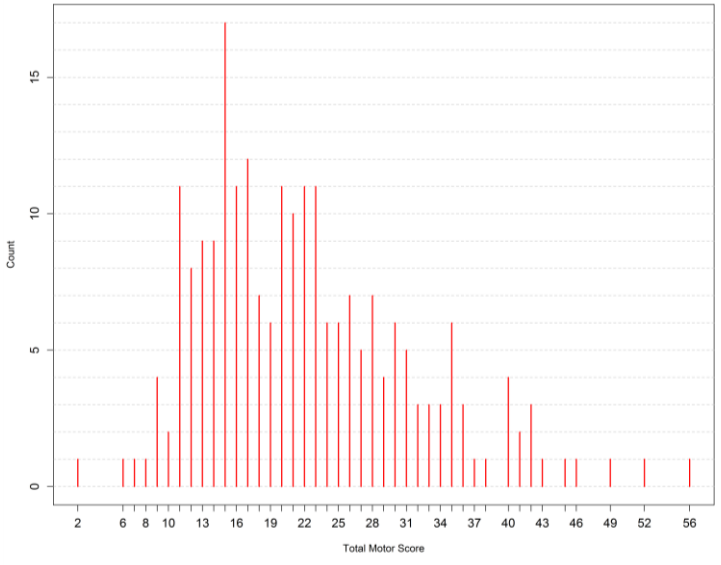

Figure S1. Count of total motor score values for converters at time of conversion.

In addition to the efforts made above to improve rater training and to query for errors, we have analyzed our normal control data for motor ratings. Table S1 below shows the 99th percentile of total motor score for our normal controls binned in to five-year age groups. The percentiles are based on a fitted linear mixed effects regression (LMER) model with only the non-gene-expanded controls. The idea was to examine what total motor scores might be candidates for cutoffs using the extremes of the distributions for each age category. We decided on the criterion that no more than 1% of controls be classified as cases and thus, our goal was to identify TMS cutoffs for this purpose. These data are consistent with those reported in the literature suggesting that minor motor abnormalities or "soft signs" are evident in a large proportion of individuals without known cerebral involvement, which increases with age. Table S1 shows the popular cutoff of total motor score=5 might be too low even for a 30-year-old, in the sense that many more than 1% of controls with no known neurologic or psychiatric syndrome would be classified as cases. Table S1 indicates that a total motor score greater than 10 has better predictive validity for the average person at risk for HD. This number corresponds to the extreme (99th percentile) of the control group distribution for age 50 and is a rough approximation for neighboring age categories. Figure S2 shows the empirical total motor score trajectories for cases (gray) and controls (red) as a function of age. The blue line is the fitted curve from the LMER model for the 99th percentile. The blue line denotes the cutoff value for each age category as shown in the aforementioned table. As expected, the total motor score increases over time with age for both groups. The variation in the CAG-expanded group is much more extreme, however. As the figure shows, the total motor scores for the controls often surpass 5 and we think a higher cutoff is appropriate. Further research and analyses like we present here are warranted.

Table S1. The 99th percentile of total motor score as a function of age, based on analysis of the non-gene-expanded controls.

Age:	30	35	40	45	50	55	60	65	70	75
Total motor score:	7	8	8	9	10	11	12	12	13	14

Figure S2. Total motor score trajectories as a function of age for gene-expanded cases (gray lines) and controls (red lines).

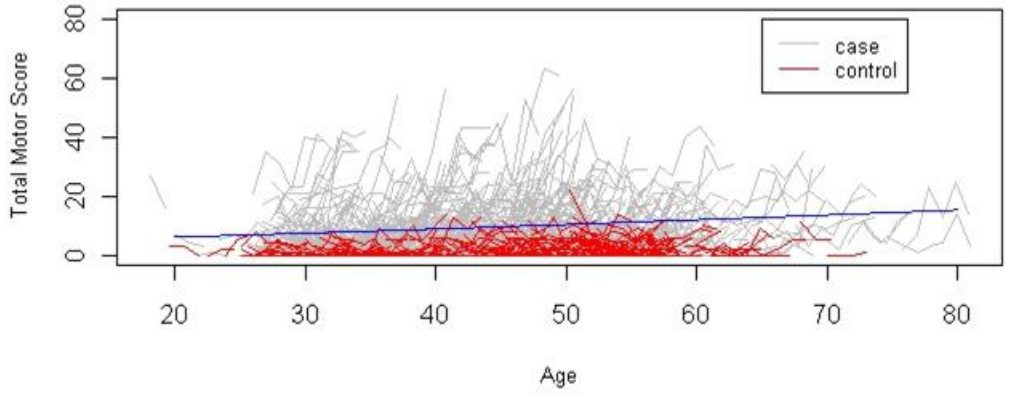

The blue line is the 99th percentile line based on the fitted linear mixed effects regression model for the controls.

Table S2. Variable descriptive statistics for gene-expanded groups (Converters, Non-Converters, Combined) at study entry.

	All Gene-Expanded				Non-Converters (Gene-Expanded)				Converters (Gene-Expanded)			
Variable	Mean	SD	Min	Max	Mean	SD	Min	Max	Mean	SD	Min	Max
Accumben	0.0003	0.0001	0.0002	0.0006	0.0003	0.0001	0.0002	0.0006	0.0003	0.0000	0.0002	0.0005
F-Apa-C	12.0385	5.2428	8.0000	38.0000	11.6989	4.9562	8.0000	38.0000	13.2754	6.0288	8.0000	37.0000
BDI	8.0122	8.7265	0.0000	48.0000	7.5664	8.2197	0.0000	47.0000	9.2605	9.9248	0.0000	48.0000
Brady	1.9329	2.3566	0.0000	17.0000	1.4965	1.9358	0.0000	12.0000	3.5778	2.9947	0.0000	17.0000
Caudate	0.0037	0.0008	0.0013	0.0062	0.0039	0.0008	0.0014	0.0062	0.0031	0.0008	0.0013	0.0055
Chorea	0.9404	1.6555	0.0000	13.0000	0.7075	1.3225	0.0000	8.0000	1.8178	2.3505	0.0000	13.0000
CSF	0.1552	0.0334	0.0462	0.2689	0.1516	0.0320	0.0462	0.2660	0.1708	0.0347	0.0919	0.2689
F-Dis-C	16.6826	5.2706	12.0000	55.0000	16.5119	5.2388	12.0000	55.0000	17.3043	5.3516	12.0000	39.0000
DCL	0.8285	0.8300	0.0000	3.0000	0.6757	0.7304	0.0000	3.0000	1.4044	0.9263	0.0000	3.0000
Dystonia	0.1062	0.4691	0.0000	6.0000	0.0825	0.3672	0.0000	3.0000	0.1956	0.7301	0.0000	6.0000
ECOG-C	1.1817	0.2437	1.0000	2.4118	1.1713	0.2278	1.0000	2.3235	1.3859	0.4276	1.0882	2.4118
ECOG-P	1.3350	0.3359	1.0000	2.7647	1.3262	0.3381	1.0000	2.7647	1.5119	0.2389	1.0882	1.8529
F-Exc-C	24.3195	9.3023	16.0000	60.0000	23.6088	8.9656	16.0000	60.0000	26.9082	10.0424	16.0000	59.0000
FAS	24.8237	0.7652	14.0000	25.0000	24.8779	0.5823	19.0000	25.0000	24.6682	1.1247	14.0000	25.0000
Globus	0.0106	0.0008	0.0084	0.0134	0.0107	0.0008	0.0084	0.0134	0.0103	0.0008	0.0088	0.0132
Hippo	0.0022	0.0002	0.0015	0.0031	0.0023	0.0003	0.0015	0.0031	0.0022	0.0002	0.0016	0.0028
EmoRec	25.3346	6.1478	5.0000	39.0000	26.1395	5.8971	8.0000	39.0000	23.0048	6.2774	5.0000	37.0000
TMS	4.8220	5.2136	0.0000	35.0000	3.8160	4.3085	0.0000	34.0000	8.6133	6.4515	0.0000	35.0000
Ocular	1.4520	2.2024	0.0000	14.0000	1.1474	1.9710	0.0000	14.0000	2.6000	2.6169	0.0000	12.0000
Putamen	0.0050	0.0010	0.0022	0.0079	0.0051	0.0009	0.0027	0.0079	0.0042	0.0009	0.0022	0.0065
Rigidity	0.3905	0.7490	0.0000	4.0000	0.3821	0.7419	0.0000	4.0000	0.4222	0.7760	0.0000	4.0000
Smell-ID	0.8392	0.0998	0.3500	1.0000	0.8533	0.0922	0.3500	1.0000	0.7877	0.1094	0.5250	1.0000
Stroop-Co	77.4220	14.0616	35.0000	135.0000	79.2122	13.6874	35.0000	135.0000	70.7467	13.4424	36.0000	114.0000
Stroop-In	44.9097	10.4630	13.0000	82.0000	46.3588	10.2985	13.0000	82.0000	39.4821	9.2363	18.0000	73.0000
Stroop-Wo	98.9211	17.5804	38.0000	155.0000	101.0226	17.2327	44.0000	155.0000	91.0756	16.6553	38.0000	142.0000
SDMT	50.5122	11.4492	16.0000	110.0000	52.1430	11.1004	23.0000	110.0000	44.4311	10.6765	16.0000	75.0000
Sp-Tapping	252.0797	54.3451	161.5300	581.5800	241.0491	42.7676	161.5300	435.0700	283.8925	69.6495	176.8500	581.5800
Dysrhythmia	51.5977	24.8441	18.9800	225.7300	46.7395	20.3450	18.9800	151.0300	65.4212	30.6766	20.2600	225.7300
S-Anx-C	49.1366	11.0890	41.0000	116.0000	48.7302	10.6786	41.0000	116.0000	50.5514	12.3351	41.0000	109.0000
S-Dep-C	52.7404	13.7361	41.0000	145.0000	51.9168	13.2688	41.0000	145.0000	55.6075	14.9338	41.0000	113.0000
TFC	12.8085	0.7117	7.0000	13.0000	12.8430	0.6720	7.0000	13.0000	12.6786	0.8333	7.0000	13.0000
Thalamus	0.0095	0.0007	0.0078	0.0120	0.0095	0.0007	0.0078	0.0118	0.0094	0.0007	0.0079	0.0120
S-Hos-C	53.3279	15.9044	42.0000	141.0000	52.5013	15.1221	42.0000	133.0000	56.2710	18.1579	42.0000	141.0000
S-OC-C	52.7582	13.4443	41.0000	131.0000	51.8360	13.0431	41.0000	131.0000	56.0421	14.3420	41.0000	111.0000
Lobar Gray	0.2429	0.0182	0.1816	0.2951	0.2447	0.0180	0.1816	0.2951	0.2354	0.0174	0.1951	0.2820
Lobar White	0.2296	0.0149	0.0992	0.3036	0.2303	0.0138	0.0992	0.3036	0.2266	0.0187	0.1087	0.2635
TMT-A	27.1190	10.4170	9.0000	138.0000	25.6391	8.6166	9.0000	65.0000	32.6044	14.0731	14.0000	138.0000
TMT-B	67.3089	33.3671	20.0000	300.0000	63.5054	29.2698	20.0000	300.0000	81.7763	42.8066	29.0000	300.0000
S-GSI-C	51.5787	13.2059	40.0000	129.0000	50.7973	12.7953	40.0000	129.0000	54.2991	14.2455	40.0000	100.0000
WHODAS-C	41.4361	6.4305	36.0000	69.0000	41.3781	6.4807	36.0000	69.0000	43.2000	4.8166	38.0000	50.0000
WHODAS-P	41.4461	8.8770	36.0000	85.0000	41.3672	9.0173	36.0000	85.0000	43.4286	3.7353	39.0000	48.0000

See "Variable descriptions" section for abbreviations

Table S3. Variable descriptive statistics for gene-expanded converters at the time of conversion.

Variable	Mean	SD	Min	Max
Accumben	0.0003	0.0001	0.0002	0.0005
F-Apa-C	15.8798	7.5888	8.0000	40.0000
BDI	10.8175	11.3832	0.0000	50.0000
Brady	8.1429	4.6353	0.0000	22.0000
Caudate	0.0028	0.0008	0.0012	0.0060
Chorea	6.3170	3.3149	0.0000	20.0000
CSF	0.1831	0.0378	0.1110	0.3000
F-Dis-C	19.4809	7.4685	12.0000	48.0000
DCL	4.0000	0.0000	4.0000	4.0000
Dystonia	1.0982	1.8724	0.0000	13.0000
ECOG-C	1.6597	0.5146	1.0000	3.7941
ECOG-P	1.6951	0.6210	1.0000	3.5882
F-Exc-C	31.1257	12.0831	16.0000	76.0000
FAS	23.6715	2.2066	14.0000	25.0000
Globus	0.0100	0.0007	0.0083	0.0123
Hippo	0.0021	0.0002	0.0016	0.0026
EmoRec	20.8916	7.4539	5.0000	39.0000
TMS	22.0804	9.3546	2.0000	56.0000
Ocular	5.6830	3.4657	0.0000	21.0000
Putamen	0.0037	0.0008	0.0026	0.0059
Rigidity	0.8393	1.2095	0.0000	6.0000
Smell-ID	0.7284	0.1511	0.2000	1.0000
Stroop-Co	64.4658	14.4778	20.0000	110.0000
Stroop-In	37.1142	10.1254	12.0000	84.0000
Stroop-Wo	80.8265	17.7626	29.0000	122.0000
SDMT	39.8676	10.6790	11.0000	66.0000
Sp-Tapping	336.5634	97.4325	210.7300	656.6300
Dysrhythmia	83.9441	36.7680	30.8800	171.1700
S-Anx-C	54.8820	16.9370	41.0000	142.0000
S-Dep-C	58.7809	16.8453	41.0000	120.0000
TFC	11.6161	1.7346	6.0000	13.0000
Thalamus	0.0092	0.0006	0.0075	0.0110
S-Hos-C	58.1277	17.0928	42.0000	130.0000
S-OC-C	62.1862	17.4341	41.0000	111.0000
Lobar Gray	0.2289	0.0182	0.1771	0.2676
Lobar White	0.2261	0.0200	0.1094	0.2665
TMT-A	36.2530	22.0434	13.0000	240.0000
TMT-B	97.1790	50.8713	27.0000	300.0000
S-GSI-C	58.8090	17.7196	40.0000	126.0000
WHODAS-C	59.9080	23.6957	36.0000	113.0000
WHODAS-P	56.9664	23.3205	36.0000	115.0000

See “Variable descriptions” section for abbreviations

Table S4. Variable descriptive statistics for controls (non-gene-expanded) at study entry.

Variable	Mean	SD	Min	Max
Accumben	0.0004	0.0001	0.0002	0.0006
F-Apa-C	11.0735	4.0370	8.0000	32.0000
BDI	4.5043	5.3282	0.0000	32.0000
Brady	1.4361	2.0237	0.0000	15.0000
Caudate	0.0043	0.0006	0.0019	0.0059
Chorea	0.2754	0.7364	0.0000	4.0000
CSF	0.1439	0.0296	0.0661	0.2907
F-Dis-C	15.9338	3.9847	12.0000	33.0000
DCL	0.4557	0.6060	0.0000	3.0000
Dystonia	0.0492	0.2706	0.0000	2.0000
ECOG-C	1.2022	0.2511	1.0000	2.2353
ECOG-P	1.2698	0.2957	1.0000	2.8125
F-Exc-C	22.0625	6.6388	16.0000	49.0000
FAS	24.9658	0.2243	23.0000	25.0000
Globus	0.0109	0.0008	0.0077	0.0129
Hippo	0.0023	0.0002	0.0015	0.0030
EmoRec	28.0913	5.1260	15.0000	40.0000
TMS	2.8000	3.4635	0.0000	25.0000
Ocular	0.7541	1.4448	0.0000	8.0000
Putamen	0.0057	0.0006	0.0035	0.0074
Rigidity	0.2852	0.6544	0.0000	3.0000
Smell-ID	0.8606	0.0940	0.3500	1.0000
Stroop-Co	81.1242	13.0372	34.0000	146.0000
Stroop-In	46.1812	9.7449	17.0000	89.0000
Stroop-Wo	102.3433	16.3259	32.0000	180.0000
SDMT	53.6000	9.3958	26.0000	83.0000
Sp-Tapping	231.4075	31.5304	147.9900	390.7400
Dysrhythmia	39.6318	15.3772	17.4900	127.3700
S-Anx-C	47.9857	11.5489	41.0000	131.0000
S-Dep-C	50.1821	11.9916	41.0000	118.0000
TFC	12.9638	0.3178	8.0000	13.0000
Thalamus	0.0096	0.0007	0.0067	0.0114
S-Hos-C	49.6157	10.5395	42.0000	119.0000
S-OC-C	49.5658	10.5872	41.0000	118.0000
Lobar Gray	0.2434	0.0182	0.1570	0.2890
Lobar White	0.2317	0.0155	0.1030	0.2676
TMT-A	25.1348	8.4655	12.0000	57.0000
TMT-B	58.7903	24.0083	24.0000	205.0000
S-GSI-C	49.5464	11.3969	40.0000	112.0000
WHODAS-C	41.4375	8.1880	36.0000	70.0000
WHODAS-P	42.6730	12.0733	36.0000	95.0000

See “Variable descriptions” section for abbreviations

Table S5. Counts of waves of annual measures (number of repeated measures) by variable (total *N*=1078).

		Waves Annual Measures (Number of Repeated Measurements)												
Variable	Domain	0 (Missing)	1	2	3	4	5	6	7	8	9	10	11	12
Brady	Motor	1	118	126	144	147	86	118	103	76	52	58	37	12
Chorea	Motor	1	118	126	144	147	86	118	103	76	52	58	37	12
Dystonia	Motor	1	118	126	144	147	86	118	103	76	52	58	37	12
TMS	Motor	1	118	126	144	147	86	118	103	76	52	58	37	12
Ocular	Motor	1	118	126	144	147	86	118	103	76	52	58	37	12
Rigidity	Motor	1	118	126	144	147	86	119	102	76	52	58	37	12
Accumbens	Imaging	90	309	268	193	129	67	20	2	0	0	0	0	0
Caudate	Imaging	90	309	268	193	129	67	20	2	0	0	0	0	0
CSF	Imaging	85	310	267	196	131	67	20	2	0	0	0	0	0
Globus	Imaging	90	309	268	193	129	67	20	2	0	0	0	0	0
Hippocampus	Imaging	90	309	268	193	129	67	20	2	0	0	0	0	0
Putamen	Imaging	90	309	268	193	129	67	20	2	0	0	0	0	0
Thalamus	Imaging	90	309	268	193	129	67	20	2	0	0	0	0	0
Lobar Gray	Imaging	101	317	263	195	131	63	8	0	0	0	0	0	0
Lobar White	Imaging	116	323	257	187	127	62	6	0	0	0	0	0	0
EmoRec	Cognitive	259	183	289	120	167	60	0	0	0	0	0	0	0
Smell-ID	Cognitive	45	210	253	140	154	110	75	65	26	0	0	0	0
Stroop-Co	Cognitive	6	121	128	150	138	89	117	97	77	59	48	37	11
Stroop-In	Cognitive	6	121	128	152	138	87	117	97	79	57	49	36	11
Stroop-Wo	Cognitive	6	121	128	149	138	90	116	97	78	59	48	37	11
SDMT	Cognitive	4	123	128	147	138	96	113	99	76	59	48	36	11
Sp-Tapping	Cognitive	258	190	289	120	164	57	0	0	0	0	0	0	0
Timing	Cognitive	264	189	282	117	168	58	0	0	0	0	0	0	0
TMT-A	Cognitive	6	175	208	171	142	121	91	62	53	39	10	0	0
TMT-B	Cognitive	6	176	214	167	143	127	81	64	51	40	9	0	0
F-Apa-C	Psychiatric	71	146	156	127	131	87	109	87	69	45	26	18	6
BDI	Psychiatric	260	90	80	112	201	115	158	62	0	0	0	0	0
F-Dis-C	Psychiatric	71	146	156	127	131	87	109	87	69	45	26	18	6
F-Exc-C	Psychiatric	71	146	156	127	131	87	109	87	69	45	26	18	6
S-Anx-C	Psychiatric	84	178	145	106	119	102	109	98	64	44	29	0	0
S-Dep-C	Psychiatric	85	178	144	106	119	102	109	98	64	44	29	0	0
S-Hos-C	Psychiatric	64	155	136	131	129	89	112	90	73	44	31	17	7
S-OC-C	Psychiatric	64	155	136	131	129	89	112	90	73	44	31	17	7
S-GSI-C	Psychiatric	84	178	145	106	119	102	109	98	64	44	29	0	0
ECOG-C	Functional	467	209	220	161	21	0	0	0	0	0	0	0	0
ECOG-P	Functional	391	193	239	220	35	0	0	0	0	0	0	0	0
FAS	Functional	249	97	81	108	207	107	164	65	0	0	0	0	0
TFC	Functional	3	119	128	143	146	87	123	93	80	57	47	40	12
WHODAS-C	Functional	539	239	201	95	4	0	0	0	0	0	0	0	0
WHODAS-P	Functional	489	195	258	128	8	0	0	0	0	0	0	0	0

See “Variable descriptions” section for abbreviations

Table S6. Converter information in other studies

Author	Year	Participants	Years	Converters	Comments
Brandt[20]	2008	49	3	21	Only cognitive predictors considered; Wisconsin Card Sort Test performance predicted diagnosis
Langbehn[22]	2007	226	4.5	58	Unified HD Rating Scale predictors considered; motor soft signs, symbol digit worse than fluency, subjective symptoms
Marder[24]	2013	211	2.5	31	PHAROS database: Mediterranean diet did not predict diagnosis
Paulsen[25]	2001	260	2	70	Huntington Study Group database: Only cognitive predictors considered; Symbol Digit Modalities Test, Stroop Color and Word Test, and verbal fluency predicted diagnosis
Snowden[26]	2002	51	5	24	Only cognitive predictors considered; Object memory, card sorting, Stroop reading, Stroop color performances predicted diagnosis
Solomon[27]	2008	43	NA	21	Only cognitive predictors considered; Reaction time, movement time, button tapping speed, and Wechsler Adult Intelligence Scale-Revised Digit Symbol Coding predicted diagnosis
Tabrizi[28]	2013	104	3	43*	TRACK-HD database; several cognitive, quantitative motor and imaging measures were predictive of conversion*

*non traditional diagnosis of total motor score=5.

Image processing

Basal ganglia structures had different imaging processing than lobar white and lobar gray. We begin with a description of the former.

Basal ganglia structures. Imaging measures included intracranial-corrected volumes for putamen, accumbens, caudate, hippocampus, thalamus, cerebral spinal fluid,[29] lobar white and gray matter.[30,31] All imaging analysis was performed at the University of Iowa Scalable Informatics, Neuroimaging, Analysis, Processing, and Software Engineering (SINAPSE) laboratory. Acquired scans are processed through a fully automated procedure, Brain Research: Analysis of Images, Networks, and Systems (BRAINS) AutoWorkup (BAW),[29] improved with SyN[32] registration from the Advanced Normalization Toolkit in the BRAINSTools software package.[a] All scans begin with visual inspection of the raw data, so only images of sufficient quality are processed. Each dataset, T1 and/or T2-weighted images, was processed together to improve the robustness of the procedure from complimentary information provided by multiple modalities. The best-rated T1-weighted image is spatially normalized to an "AC-PC" alignment, where the anterior commissure is located at physical location (0,0,0) based on prominent landmarks in MRI, including anterior and posterior commissure, and mid-sagittal plane.[33] The remaining scans acquired in the same session are then rigidly aligned to the spatially normalized T1 image, and simultaneously processed by the automated bias-field correction (ABC) algorithm, BRAINSABC.[34] For each given modality, BRAINSABC produces an average of independently bias-field corrected MR images resampled in 1mm x 1mm x 1mm, and their respective corresponding 17 tissue probability maps, including white matter, grey matter, and CSF. At this point, all longitudinal scan sessions for a single subject are used jointly to build a subject-specific atlas. The subject-specific atlas best represents the average longitudinal shape for that subject with respect to minimum mean square error of spatial displacement to each time point. This joint session template building step is used to maximize consistency by regularizing inherent scanner variation in longitudinal studies. The resulting data set of bias-corrected average T1 and/or T2 images are subsequently segmented for subcortical structures using an automated segmentation framework, BRAINSCut. BRAINSCut is an extension of previous work that now employs robust random forest machine learning that has been validated on multi-site MR data.[b,35] The subcortical structures of interest include nucleus

[a] "BRAINSTool Package". (https://github.com/BRAINSia/BRAINSTools).

[b] Kim, E. Y., Magnotta, V. A., Johnson, H.J., et al. (2014). Automated Segmentation Framework: Determining Robust Machine-Learning Algorithm and Intensity Normalization for Scalable Brain MRI. Submitted for review.

accumbens, caudate, putamen, hippocampus, and thalamus. The results of this procedure were again visually inspected and resulted in a success rate greater than 90%. All the development processing was blinded to clinical data, such as HD gene-expansion status, gender, and age.

Lobar white and lobar gray. To extract reliable volumetric segmentations, images were automatically processed with the longitudinal stream[36] in FreeSurfer which is documented and freely available for download (http://surfer.nmr.mgh.harvard.edu/). Specifically, an unbiased within-subject template space and image is created using robust, inverse consistent registration.[37] Several processing steps, such as skull stripping, Talairach transforms, atlas registration spherical surface maps and parcellations are then initialized with common information from the within-subject template, significantly increasing reliability and statistical power.[36] The technical details of these procedures are described in prior publications. [30, 36-48] Briefly, this processing includes removal of non-brain tissue using a hybrid watershed/surface deformation procedure,[48] automated Talairach transformation, segmentation of the subcortical white matter and deep gray matter volumetric structures,[30,42] intensity normalization,[49] tessellation of the gray matter white matter boundary, automated topology correction,[41,50] and surface deformation following intensity gradients to optimally place the gray/white and gray/cerebral spinal fluid borders at the location where the greatest shift in intensity defines the transition to the other tissue class.[38-40] FreeSurfer morphometric procedures have been demonstrated to show good test-retest reliability across scanner manufacturers and across field strengths.[36,46]

Statistical analysis

Joint model. The longitudinal markers considered in the analysis were collected on the participants under study and were hypothesized to be related to motor diagnosis, the event of interest. When a marker's path is directly informative about the time to the event, it is known as an endogenous covariate.[51] The Cox model and its extensions cannot properly handle endogenous covariates.[52] Therefore, joint modeling of longitudinal and time-to-event data was used for the main analysis.[53] The joint model consists of a linear mixed effect regression (LMER) component for the longitudinal marker and a Cox regression model for the time-to-event (time to motor diagnosis or censoring). In this analysis, the time metric for both portions was age scaled by corrected CAG length, which is the CAG-Age Product (CAP; see main article text). The LMER portion was a cubic spline model[54] with five knots consisting of the 1st, 25th, 50th, 75th, and 99th CAP percentiles. Two joint models were fit for every variable: (1) a reduced joint model that had only random intercepts in the LMER portion, and (2) a full joint model that included random intercepts and random slopes. The Cox model always included the covariates of gender and education, and additional covariates were added depending on the type of response variable (see below).

Reduced model. The reduced model used random intercepts to predict the hazard controlling for the covariates, indicating the conditional association between the individual deviations from the mean variable level at baseline CAP=290 and the instantaneous rate of motor diagnosis (see main text for why CAP=290 was selected as the baseline).

Suppose Y_{ij} is the response for the ith person (i=1, …, N) at the jth time point (j=1, …, n_i). Further assume that measurement Y_{ij} is taken at CAP equal to CAP_{ij}. Let $f_k(CAP_{ij})$ denote the kth natural spline basis function (k=1, …, 6). Then the cubic spline LMER model was

$$Y_{ij} = (\beta_0 + b_{0i}) + \sum_{k=1}^{6} \beta_k f_k(CAP_{ij}) + \epsilon_{ij}$$

where β denotes a fixed effect, β_0 is the fixed intercept, b_{0i} is the random intercept, and ϵ_{ij} is random (possibly measurement) error. It is assumed that the random effect is normally distributed with zero mean and non-zero variance, and it is uncorrelated with the random error that also is normally distributed with zero mean and non-zero variance over time. The Cox hazard model was

$$h_i(CAP) = h_0(CAP)exp\{\alpha_1 gender_i + \alpha_2 educ_i + \gamma_0 b_{0i}\}$$

It is assumed that right-censoring is non-informative and that the hazards are proportional (evaluation of the proportional hazards assumption is discussed below). Note the LMER and Cox models are linked by the common random intercept term, b_{0i}.

Full model. The full model used random intercepts and random spline coefficients to predict the hazard, which represented the association between the subjects' deviation from the population mean trajectory over a range of times (not just CAP=290) and the instantaneous rate of motor diagnosis. For the full model, the LMER equation was

$$Y_{ij} = (\beta_0 + b_{0i}) + (\beta_1 + b_{1i}) f_1(CAP_{ij}) + \sum_{k=2}^{6} \beta_k f_k(CAP_{ij}) + \epsilon_{ij}$$

It is assumed that the random effects have a joint-normal distribution with zero-mean vector and positive-definite variance-covariance matrix, and the random effects are uncorrelated with the normally distributed random error. The Cox model was

$$h_i(CAP) = h_0(CAP)exp\{\alpha_1 gender_i + \alpha_2 educ_i + \gamma_{01}(b_{0i} + b_{1i} f_1(CAP))\}$$

Based on the selected knots, the first natural spline basis function, $f_1(CAP_{ij})$, had non-zero values up to the third quantile of the CAP distribution. This constituted the range over which the hazard could be modified by the subject-specific deviation from the mean trajectory (i.e., by b_{1i}).

In the joint model, the deviation of the longitudinal marker either at CAP=290 (reduced model) or the deviation over a range of CAP (full model) is used to predict the hazard, and the gamma association parameter (γ) represents the variable's prediction effect. Because CAP is a form of age adjusted for CAG expansion, variables with a statistically significantly γ account for variability in the timing of diagnosis over and above CAG expansion and age (see Figure 2 of the main article text). When γ_0 (or γ_{01}) has a positive sign, a given individual with a higher score has an increased risk of motor diagnosis relative to another given individual with a lower score. When γ_0 (or γ_{01}) has a negative sign, a given individual with a lower score has an increased risk of motor diagnosis. To facilitate the comparison of the gamma coefficients among the variables, each variable was scaled to zero mean and unit variance using the mean and standard deviation (SD) among all the participants and all the time points. The standardization indicates that γ_0 (or γ_{01}) is the effect on the hazard for a one standard deviation (1SD) difference among two given individuals (controlling for the covariates).

The joint model was estimated using maximum likelihood methods (the parameters of the LMER and Cox models are simultaneously estimated). Standard errors (SE) were calculated using a bootstrap procedure in which the original data was resampled with replacement and the models refitted (participants' repeated measures matrices were resampled). The hazard ratio (HR) for each model was computed as exp(γ_0) or exp(γ_{01}) and represented the multiplicative increase in risk attributable to the level of the longitudinal variable, either deviations from the group mean at CAP = 290 (reduced model), or deviations from the mean trajectory over a range of CAP (full model). When $\gamma_0 < 0$ or $\gamma_{01} < 0$, HR^{-1} was used as the effect size. The bootstrap SE was used to compute an approximate 95% confidence interval (CI) and a *Z*-test of the null hypothesis that the gamma parameter is zero (no association). The covariates in all models were gender and education. If a longitudinal variable was from the cognitive domain, then depression was added as a covariate because of evidence that mood affects cognitive performance. If a longitudinal variable was an imaging variable, then field strength (1·5T, 3T) was added as a covariate because some sites updated their scanners during the study.[55] The HR or HR^{-1} was the primary effect size and the variables were rank-ordered based on the absolute *Z*-value for γ_{01} (full model).

Cumulative hazard profiles. A subsequent analysis was performed to characterize the risk of motor diagnosis over the lifespan with and without predictor information (see Figure 2 of the text). Individual fitted values at CAP=290 from the LMER spline model for each variable were used in a separate (not joint) Cox model to predict time of diagnosis for the span of CAP>290. The Cumulative hazard as a function of CAP was estimated based on the fitted Cox model.[56]

Proportional hazards assumption. The proportional hazards assumption was evaluated by examining plots of the scaled Schoenfeld residuals by log CAP for each variable based on the cross-sectional Cox model described in the last section. A statistical test of proportional hazards was also conducted for each variable.[57] Both the residual plots and statistical tests indicated that the proportional hazards assumption was reasonable for the analysis. None of the global tests were statistically significant and the residual plots did not show extreme non-linearity or other irregularities.

Computer software. All analysis was performed with the `R` computer software.[58] Joint modeling was accomplished using the `joineR` package,[59] cross-sectional Cox modeling and proportionality testing was carried out using the `survival` package,[56] spline fitting was performed with the `gamm4` package,[60] and the `lme4` package was used for additional LMER modeling (Bates et al., 2014).[61]

References

1 Huntington Study Group. Unified Huntington's Disease Rating Scale: reliability and consistency. *Mov Disord* 1996; **11**(2): 136–42.

2 Wechsler D. Manual for the Wechsler Adult Intelligence Scale - Revised. New York, NY: Psychological Corporation; 1981.

3 Lezak MD, Howieson D, Loring D. Neuropsychological assessment. 4th ed. New York: Oxford University Press; 2004. xiv, 1016 p.

4 Smith A. Symbol Digit Modalities Test (SDMT) Manual (Revised). Los Angeles, CA: Western Psychological Services; 1982.

5 Stroop JR. Studies of interference in serial verbal reactions. *J Exp Psychol* 1935; **18**: 643–62.

6 Golden C. Stroop Color and Word Test: Cat. No. 30150M; a Manual for Clinical and Experimental Uses. Chicago, IL: Stoelting; 1978.

7 Rowe KC, Paulsen JS, Langbehn DR, et al. Self-paced timing detects and tracks change in prodromal Huntington disease. *Neuropsychology* 2010; **24**(4): 435–42.

8 Doty RL, Shaman P, Kimmelman CP, Dann MS. University of Pennsylvania Smell Identification Test: a rapid quantitative olfactory function test for the clinic. *Laryngoscope* 1984; **94**(2 Pt 1): 176–8.

9 O'Rourke JJ, Beglinger LJ, Smith MM, et al. The Trail Making Test in prodromal Huntington disease: contributions of disease progression to test performance. *J Clin Exp Neuropsychol* 2011; **33**(5): 567–79.

10 Reitan R. Validity of the trail making test as an indicator of organic brain damage. *Percept Mot Skills* 1958; **8**: 271–76.

11 Johnson SA, Stout JC, Solomon AC, et al. Beyond disgust: impaired recognition of negative emotions prior to diagnosis in Huntington's disease. *Brain* 2007; **130**(Pt 7): 1732–44.

12 Ekman P, Friesen WV. Measuring Facial Movement. *Environmental Psychology and Nonverbal Behavior* 1976; **1**(1): 56–75.

13 Aylward EH, Nopoulos PC, Ross CA, et al. Longitudinal change in regional brain volumes in prodromal Huntington disease. *J Neurol Neurosurg Psychiatry* 2011; **82**(4): 405–10.

14 Farias ST, Mungas D, Reed BR, et al. The measurement of everyday cognition (ECog): scale development and psychometric properties. *Neuropsychology* 2008; **22**(4): 531–44.

15 World Health Organization. World Health Organization Psychiatric Disability Assessment Schedule (WHO/DAS), with a Guide to Its Use. Geneva, Switzerland: World Health Organization; 1988.

16 Derogatis L. Administration, scoring & procedures manual-I for the revised version and other instruments of the psychopathology rating scale series. Baltimore, MD: John Hopkins University; 1977.

17 Grace J, Malloy P. Frontal systems behavior scale: professional manual. Lutz, FL: Psychological Assessment Resources, Incorporated; 2000. 109 p.

18 Beck A, Steer R, Brown G. Beck Depression Inventory-II (BDI-II): Manual for Beck Depression Inventory-II: Pearson; 1993.

19 Aylward EH, Liu D, Nopoulos PC, et al. Striatal volume contributes to the prediction of onset of Huntington disease in incident cases. *Biol Psychiatry* 2012; **71**: 822-8.

20 Brandt J, Inscore AB, Ward J, et al. Neuropsychological deficits in Huntington's disease gene carriers and correlates of early "conversion". *J Neuropsychiatry Clin Neurosci* 2008; **20**: 466-72.

21 Harrington DL, Smith MM, Zhang Y, Carlozzi NE, Paulsen JS, PREDICT-HD Investigators of the Huntington Study Group. Cognitive domains that predict time to diagnosis in prodromal Huntington disease. *J Neurol Neurosurg Psychiatry* 2012; **83**: 612-9.

22 Langbehn DR, Paulsen JS, Huntington Study Group. Predictors of diagnosis in Huntington disease. *Neurology* 2007; **68**: 1710-7.

23 Long JD, Paulsen JS, Marder K, et al. Tracking motor impairments in the progression of Huntington's disease. *Mov Disord* 2014; **29**: 311-9.

24 Marder K, Gu Y, Eberly S, et al. Relationship of Mediterranean diet and caloric intake to phenoconversion in Huntington disease. *JAMA Neurol* 2013; **70**: 1382-8.

25 Paulsen JS, Zhao H, Stout JC, et al. Clinical markers of early disease in persons near onset of Huntington's disease. *Neurology* 2001; **57**: 658-62.

26 Snowden JS, Craufurd D, Thompson J, Neary D. Psychomotor, executive, and memory function in preclinical Huntington's disease. *J Clin Exp Neuropsychol* 2002; **24**: 133-45.

27 Solomon AC, Stout JC, Weaver M, et al. Ten-year rate of longitudinal change in neurocognitive and motor function in prediagnosis Huntington disease. *Mov Disord* 2008; **23**: 1830-6.

28 Tabrizi SJ, Scahill RI, Owen G, et al. Predictors of phenotypic progression and disease onset in premanifest and early-stage Huntington's disease in the TRACK-HD study: analysis of 36-month observational data. *Lancet Neurol* 2013; **12**: 637-49.

29 Pierson R, Johnson H, Harris G, et al. Fully automated analysis using BRAINS: AutoWorkup. *Neuroimage* 2011; **54**(1): 328–36.

30 Fischl B, Salat DH, Busa E, et al. Whole brain segmentation: automated labeling of neuroanatomical structures in the human brain. *Neuron* 2002; **33**(3): 341–55.
31 Fischl B. FreeSurfer. *Neuroimage* 2012; 62(2): 774–81.
32 Avants BB, Epstein CL, Grossman M, Gee JC. Symmetric diffeomorphic image registration with cross-correlation: evaluating automated labeling of elderly and neurodegenerative brain. *Med Image Anal* 2008; **12**(1): 26–41.
33 Ghayoor A, Vaidya JG, Johnson H. Development of a novel constellation based landmark detection algorithm. *Proc SPIE Medical Imaging* 2013; **8669** (86693F-6).
34 Young Kim E, Johnson HJ. Robust multi-site MR data processing: iterative optimization of bias correction, tissue classification, and registration. Front Neuroinform 2013; 7: 29.
35 Powell S, Magnotta VA, Johnson H, Jammalamadaka VK, Pierson R, Andreasen NC. Registration and machine learning-based automated segmentation of subcortical and cerebellar brain structures. *Neuroimage* 2008; **39**(1): 238–47.
36 Reuter M, Schmansky NJ, Rosas HD, Fischl B. Within-subject template estimation for unbiased longitudinal image analysis. *Neuroimage* 2012; **61**(4): 1402–18.
37 Reuter M, Rosas HD, Fischl B. Highly accurate inverse consistent registration: a robust approach. *Neuroimage* 2010; **53**(4): 1181–96.
38 Dale AM, Fischl B, Sereno MI. Cortical surface-based analysis. I. Segmentation and surface reconstruction. *Neuroimage* 1999; **9**(2): 179–94.
39 Dale AM, Sereno MI. Improved Localizadon of Cortical Activity by Combining EEG and MEG with MRI Cortical Surface Reconstruction: A Linear Approach. *J Cogn Neurosci* 1993; **5**(2): 162–76.
40 Fischl B, Dale AM. Measuring the thickness of the human cerebral cortex from magnetic resonance images. *Proc Natl Acad Sci U S A* 2000; **97**(20): 11050–5.
41 Fischl B, Liu A, Dale AM. Automated manifold surgery: constructing geometrically accurate and topologically correct models of the human cerebral cortex. *IEEE Trans Med Imaging* 2001; **20**(1): 70–80.
42 Fischl B, Salat DH, van der Kouwe AJ, et al. Sequence-independent segmentation of magnetic resonance images. *Neuroimage* 2004; **23 Suppl 1**: S69–84.
43 Fischl B, Sereno MI, Dale AM. Cortical surface-based analysis. II: Inflation, flattening, and a surface-based coordinate system. *Neuroimage* 1999; **9**(2): 195–207.
44 Fischl B, Sereno MI, Tootell RB, Dale AM. High-resolution intersubject averaging and a coordinate system for the cortical surface. *Hum Brain Mapp* 1999; **8**(4): 272–84.
45 Fischl B, van der Kouwe A, Destrieux C, et al. Automatically parcellating the human cerebral cortex. *Cereb Cortex* 2004; **14**(1): 11–22.
46 Han X, Jovicich J, Salat D, et al. Reliability of MRI-derived measurements of human cerebral cortical thickness: the effects of field strength, scanner upgrade and manufacturer. *Neuroimage* 2006; **32**(1): 180–94.
47 Jovicich J, Czanner S, Greve D, et al. Reliability in multi-site structural MRI studies: effects of gradient non-linearity correction on phantom and human data. *Neuroimage* 2006; **30**(2): 436–43.
48 Segonne F, Dale AM, Busa E, et al. A hybrid approach to the skull stripping problem in MRI. *Neuroimage* 2004; **22**(3): 1060–75.
49 Sled JG, Zijdenbos AP, Evans AC. A nonparametric method for automatic correction of intensity nonuniformity in MRI data. *IEEE Trans Med Imaging* 1998; **17**(1): 87–97.
50 Segonne F, Pacheco J, Fischl B. Geometrically accurate topology-correction of cortical surfaces using nonseparating loops. *IEEE Trans Med Imaging* 2007; **26**(4): 518–29.
51 Kalbfleisch JD, Prentice RL. The statistical analysis of failure time data. 2nd ed. Hoboken, N.J.: J. Wiley; 2002. xiii, 439 p.
52 Rizopoulos D. Joint models for longitudinal and time-to-event data : with applications in R. Boca Raton: CRC Press; 2012. xiv, 261 p.
53 Wulfsohn MS, Tsiatis AA. A joint model for survival and longitudinal data measured with error. *Biometrics* 1997; **53**(1): 330–9.
54 De Boor C. A practical guide to splines : with 32 figures. Rev. ed. New York: Springer; 2001. xviii, 346 p.
55 Jovicich J, Czanner S, Han X, et al. MRI-derived measurements of human subcortical, ventricular and intracranial brain volumes: Reliability effects of scan sessions, acquisition sequences, data analyses, scanner upgrade, scanner vendors and field strengths. *Neuroimage* 2009; 46(1): 177–92.
56 Therneau TM, Grambsch PM. Modeling survival data : extending the Cox model. New York: Springer; 2000. xiii, 350 p.
57 Grambsch PM, Therneau TM. Proportional Hazards Tests and Diagnostics Based on Weighted Residuals. *Biometrika* 1994; **81**: 515-26.
58 R Development Core Team. R: A language and environment for statistical computing. R Foundation for Statistical Computing. Vienna, Austria. ISBN 3-900051-07-0. 2014. Available from: http://www.R-project.org.

59 Philipson P, Sousa I, Diggle P, Williamson P, Kolamunnage-Dona R, Henderson R. joineR: Joint modelling of repeated measurements and time-to-event data. 2012. Available from: http://CRAN.R-project.org/package=joineR.
60 Wood S, Scheipl F. gamm4: Generalized additive mixed models using mgcv and lme4. 2014. Available from: http://CRAN.R-project.org/package=gamm4
61 Bates D, Maechler M, Bolker B, Walker S. _lme4: Linear mixed-effects models using Eigen and S4_2014. Available from: http://CRAN.R-project.org/package=lme4.

Study groups

Executive Committee
Jane S. Paulsen, Principal Investigator, Jeffrey D. Long, Hans J. Johnson, Thomas Brashers-Krug, Phil Danzer, Amanda Miller, H. Jeremy Bockholt, and Kelsey Montross (University of Iowa).
Scientific Consultants
Deborah Harrington (University of California, San Diego); Holly Westervelt (Rhode Island Hospital/Alpert Medical School of Brown University); Elizabeth Aylward (Seattle Children's Research Institute); David J. Moser, Janet Williams, Nancy Downing, Vincent A. Magnotta, Jatin Vaidya, Daniel O'Leary, and Kim Eun Young (University of Iowa); Stephen Rao (Cleveland Clinic).
Core Sections
Biostatistics: Jeffrey D. Long, Ji-In Kim, Spencer Lourens (University of Iowa); Ying Zhang, and Wenjing Lu (University of Indiana).
Ethics: Cheryl Erwin (Texas Tech University Health Sciences Center); Thomas Brashers-Krug and Janet Williams (University of Iowa); Martha Nance (University of Minnesota).
Biomedical Informatics: H. Jeremy Bockholt, Jason Evans, and Roland Zschiegner (University of Iowa).